

## Lightning on Jupiter observed in the $H_{\alpha}$ line by the Cassini imaging science subsystem

Ulyana A. Dyudina<sup>a,\*</sup>, Anthony D. Del Genio<sup>a</sup>, Andrew P. Ingersoll<sup>b</sup>, Carolyn C. Porco<sup>c</sup>,  
Robert A. West<sup>d</sup>, Ashwin R. Vasavada<sup>c</sup>, John M. Barbara<sup>a</sup>

<sup>a</sup> NASA/Goddard Institute for Space Studies, 2880 Broadway, New York, NY 10025, USA

<sup>b</sup> 150-21, Geological and Planetary Sciences, Caltech, Pasadena, CA 91125, USA

<sup>c</sup> Space Science Institute, 4750 Walnut Street, Suite 205, Boulder, CO 80301, USA

<sup>d</sup> Jet Propulsion Laboratory, California Institute of Technology, 4800 Oak Grove Drive, Pasadena, CA 91109, USA

<sup>e</sup> Department of Earth and Space Sciences, University of California, Los Angeles, CA 90095-1567, USA

Received 18 May 2003; revised 18 July 2004

Available online 11 September 2004

### Abstract

Night side images of Jupiter taken by the Cassini Imaging Science Subsystem (ISS) camera with the  $H_{\alpha}$  filter reveal four lightning clusters; two of them are repeated observations of the same storm. All of these flashes are associated with storm clouds seen a few hours earlier on the day side of Jupiter. Some of the clouds associated with lightning do not extend to the upper troposphere. The repeated lightning observations taken 20 hr apart show that storm clouds, whose mean lifetime is  $\sim 4$  days, are electrically active during a large fraction of their lifetime. The optical power of the lightning detected with the  $H_{\alpha}$  filter compared to the clear-filter power of Galileo lightning may indicate that the  $H_{\alpha}$  line in the lightning spectrum is about ten times weaker than expected, consistent with a flat spectrum having no prominent  $H_{\alpha}$  line. This may suggest that lightning is generated in atmospheric layers deeper than 5 bars. This, in turn, may suggest that the water abundance of the jovian interior is more than  $1 \times$  solar. Averaged over many flashes, the most powerful Cassini lightning storm emits  $0.8 \times 10^9$  W in the  $H_{\alpha}$  line, which implies  $4 \times 10^{10}$  W of broadband optical power. This is 10 times more powerful than the most intense jovian lightning observed before by Voyager 2.

© 2004 Elsevier Inc. All rights reserved.

*Keywords:* Jupiter, atmosphere; Atmospheres, composition; Meteorology; Spectroscopy

### 1. Introduction

Understanding lightning on Jupiter is interesting for several reasons. Obviously, knowing of powerful thunderstorms on another planet is interesting by itself. Less obviously, lightning is diagnostic of dynamics, chemical composition, and heat exchange within the jovian atmosphere. Lightning-derived information is especially important for studying the jovian atmosphere below the 5-bar pressure level because few other remote sensing techniques can reach down to these cloud-covered depths.

Cassini observed lightning on Jupiter with a narrow-band (11 nm-wide) filter spanning the main feature of the laboratory-simulated jovian lightning spectrum—the  $H_{\alpha}$  emission line (Borucki et al., 1996). This wavelength is different from that of all previous lightning detections by the Voyagers (Smith et al., 1979; Cook et al., 1979; Magalhães and Borucki, 1991) and Galileo (Little et al., 1999; Gierasch et al., 2000), which observed lightning with broad-band filters in visible wavelengths. Reviews of previous jovian lightning observations can be found in Williams et al. (1983), Uman (1987), Desch et al. (2002), and Rakov and Uman (2003).

In this paper we compare the optical power and number of lightning storms detected by Cassini  $H_{\alpha}$  observations

\* Corresponding author. Fax: (212)-678-5552.

E-mail address: [ulyana@gps.caltech.edu](mailto:ulyana@gps.caltech.edu) (U.A. Dyudina).

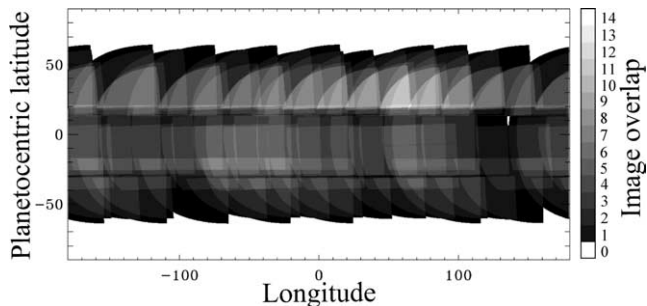


Fig. 1. Area surveyed by the nightside  $H_{\alpha}$  observations of Cassini ISS. The greyscale indicates the number of overlapping Cassini images ranging from 1 (dark grey) to the maximum overlap of 14 images (white). Non-surveyed areas are also shown in white.

with the optical power and number of lightning storms detected by Galileo broad-band observations (Section 2). We argue that the  $H_{\alpha}$  line in the lightning spectrum is unexpectedly weak, implying that lightning is deeper than 5 bars and thus that the water abundance in the jovian interior is more than  $1 \times$  solar (Section 3.1). We report on the location and appearance of four lightning clusters and day-side convective clouds corresponding to each of the four clusters (Section 3.2). We compare the optical power of Cassini and Galileo lightning with Voyager 2 lightning in Section 3.3. We also discuss the application of these results to the prospective Cassini lightning search on Saturn (Section 4).

## 2. Data

The Cassini camera (Imaging Science Subsystem, or ISS; (Porco et al., 2003)) performed the largest ever survey of the nightside of Jupiter in its search for lightning. Figure 1 shows the area surveyed by Cassini. To estimate the total area surveyed we added the areas of all images, including repeated observations of the same location. This gives  $2.14 \times 10^{11}$  km<sup>2</sup>, about three times the jovian surface area. Without counting repeated observations, the survey includes 0.87 of the planet’s surface. About half of the survey occurred near the closest approach on December 31, 2000–January 1, 2001. Another half occurred on January 10–11, 2001.

Cassini observed lightning from a distance of 140–200 jovian radii ( $R_J$ ), much farther from Jupiter than Voyager 1 ( $5R_J$ ), Voyager 2 ( $13R_J$ ) or Galileo (16–93 $R_J$ ). This greater distance was expected to increase the light scattered from outside the camera’s field of view because the bright jovian crescent appeared closer to the camera’s axis. The moonlit clouds on the jovian nightside were much fainter than the light scattered inside the camera and did not contribute substantially to the background illumination. To diminish the scattered light the lightning search was performed with the narrow-band  $H_{\alpha}$  filter.

Figure 2 illustrates how the  $H_{\alpha}$  filter can help combat scattered light. Jovian lightning simulated in the laboratory (Borucki et al., 1996) has a prominent  $H_{\alpha}$  line (black and red curves). The solar spectrum is nearly flat over this range and

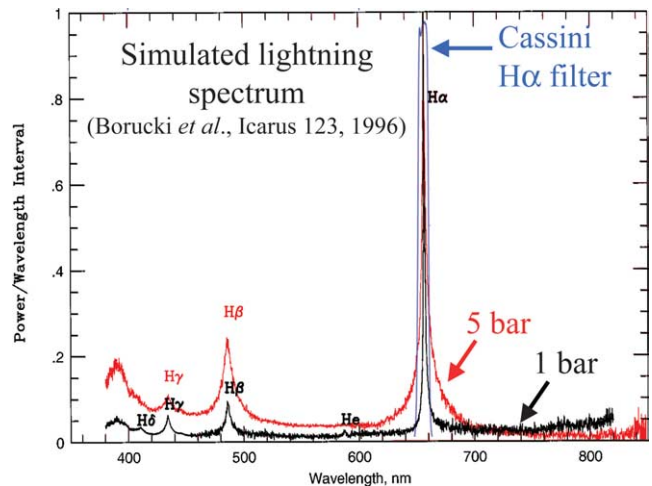


Fig. 2. Simulated spectrum of jovian lightning obtained in the laboratory by Borucki et al. (1996) compared with Cassini  $H_{\alpha}$  filter transmissivity. Spectrum of lightning at 1 bar is shown in black. Spectrum of lightning at 5 bars is shown in red. Both spectra are normalized by the brightest line ( $H_{\alpha}$ ). Cassini  $H_{\alpha}$  filter transmissivity is shown in blue.

has a small minimum at  $H_{\alpha}$ . Because of such spectra, images taken with the narrow  $H_{\alpha}$  filter are expected to have a better ratio of lightning brightness to the brightness of scattered light, which has a solar spectrum. Convolved with the simulated spectra in Fig. 2, the  $H_{\alpha}$  filter intercepts 23% of the 380–820 nm energy for the 1-bar lightning and 16% of the 380–820 nm energy for the 5-bar lightning.

Cassini observations were planned according to the Galileo and Voyager estimates for lightning brightness and according to the estimates above for the  $H_{\alpha}$  filter efficiency. Surprisingly, Cassini detected very few instances of lightning, i.e., only four clusters instead of an order of tens to hundreds expected (see below). Apparently, the rest of the lightning is too faint and falls below the ISS detection limit. The actual strength of the  $H_{\alpha}$  line for jovian lightning had never been directly observed. We propose that the small number of lightning detections is due to the weakness of the  $H_{\alpha}$  line compared to the laboratory simulations for 1- and 5-bar lightning. Comparing Cassini  $H_{\alpha}$  and Galileo broadband observations we estimate the strength of the  $H_{\alpha}$  line needed to explain the number of lightning spots detected by both observations. No night-side images were taken by Cassini with a broadband filter near the closest approach, and only near the closest approach is the spatial resolution of the images high enough to detect lightning. Because of that to compare the number of lightning events per unit area seen by Cassini through the  $H_{\alpha}$  filter with analogous observations through a broadband filter we use the 29 Galileo lightning storms. These storms were observed on Galileo orbits C10, E11 (Little et al., 1999), and orbit C20 (storms described in Gierasch et al. (2000) and two other C20 storms).

While comparing Cassini and Galileo lightning frequencies we assume no change in the global average lightning frequency from the Galileo to the Cassini observing time. This assumption is based on the very similar estimates

of optical lightning power per unit area for Voyager 2 in 1979 ( $0.32 \times 10^{-6} \text{ W/m}^2$ ) and Galileo in 1997 ( $0.30 \times 10^{-6} \text{ W/m}^2$ ) (Little et al., 1999). Our lightning rate stability assumption is also supported by the similar appearance of jovian clouds between Voyagers (1979), Galileo (1997 and 1999), and Cassini (2001) lightning observations. About an order of magnitude decrease in global lightning frequency during the 2–4 years between Galileo and Cassini may be an alternative explanation to our  $H_\alpha$  strength hypothesis. Long-term monitoring of the jovian nightside or a direct lightning spectrum observation (both only possible from a spacecraft) may help resolve this issue.

Another objective of the Cassini lightning survey was to study the day-side appearance of jovian lightning storms, some of which are seen as small bright clouds in Voyager and Galileo day-side images. To see the day-side clouds, Cassini imaged the illuminated jovian crescent a few hours before the area rotated onto the night side and was surveyed for lightning.

### 2.1. Photometric analysis

To estimate the strength of the  $H_\alpha$  line in the lightning spectrum, we make a prediction for the number of lightning spots, which Cassini should see given the Galileo lightning distribution. We define the  $H_\alpha$  line strength  $L_{H_\alpha}$  as a ratio between the lightning energy spanned by the Cassini  $H_\alpha$  filter to the lightning energy spanned by the broad-band Galileo clear filter. The stronger the  $H_\alpha$  line is the brighter the Cassini lightning images should be.

First we estimate the geometric size and brightness of the Galileo lightning. To do that we estimate the radiation intensities  $I$  (units of  $\text{W}/(\text{m}^2 \text{sr})$ ) for the Galileo lightning spots, defined as follows.

$$I \equiv \int_{\text{CLR}} I_\lambda d\lambda, \quad (1)$$

where  $I_\lambda$  is the specific intensity (as defined in Goody and Yung (1989)). The wavelength dependence of  $I_\lambda$  is the unknown spectrum of jovian lightning. CLR denotes the effective width of the Galileo clear filter (385–935 nm, slightly wider than the 380–820 span of the Borucki et al. (1996) spectrum in Fig. 2).

We derive the intensity for each of the 23- to 134-km-wide pixels in the Galileo lightning spots. Following Little et al. (1999), we convert the raw data numbers (DN) into intensity  $I$ :

$$I = (\text{DN} - \text{DN}_b) \Delta\lambda / (S \cdot \text{Exp}). \quad (2)$$

Here  $\text{DN}_b$  is the background data number,  $\Delta\lambda$  is the width of the relevant filter, 550 nm for clear (CLR), 80 nm for green (GRN), 80 nm for RED, 45 nm for violet (VLT), Exp is the exposure time, and  $S$  is the camera sensitivity for the relevant mode and gain state.  $S = S_{\text{HIM},g_2} \cdot g_2 / (g_i \cdot r)$ , where  $S_{\text{HIM},g_2}$  is the band-averaged sensitivity for the non-summed

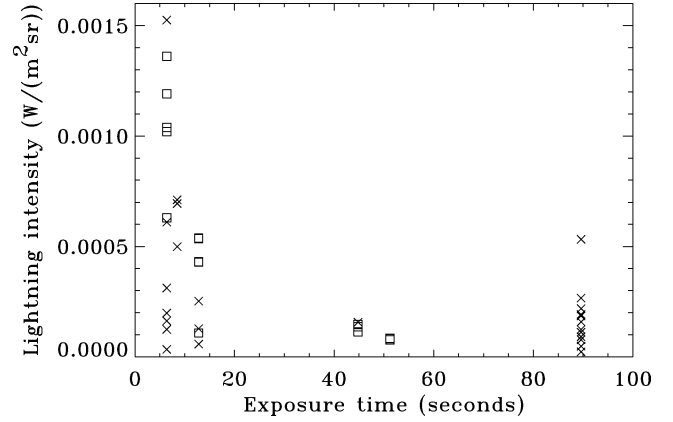


Fig. 3. Brightest pixel intensity of the Galileo lightning spots  $I$  calculated as steady light sources plotted versus exposure time. Only lightning seen through the clear filter appears on this plot. Open squares denote saturated lightning spots, at which the actual intensity is larger than the value on the plot. X-symbols denote non-saturated lightning spots, where the intensity is an accurate estimate.

gain 2 (see the column labeled Earth-2 in Table 3 of Klaasen et al. (1997)),  $r$  is the summation factor ( $r = 1$  for non-summed and  $r = 0.1997$  for summed pixels), and  $g_i$  is the gain state ratio factor for the  $i$ th gain state (Klaasen et al., 1997).

Note that we assume the storms to be steady light sources and neglect the flickering nature of lightning. This steady-source approach is good to first order for long (tens of seconds) exposures because the storms are flashing approximately every 5 s (Little et al., 1999; Dyudina et al., 2002). However, 21 out of 53 Galileo lightning spots have short exposures (6.4, 8.5, or 12.8 s). We assume these spots to be steady light sources as well. The intensity for these spots may be overestimated because unusually bright lightning may have been accidentally observed during the short exposures.

Figure 3 shows how Galileo lightning intensities (calculated as steady sources) depend on the exposure times. Some lightning spots are saturated. The corresponding open squares in Fig. 3 give a lower estimate for the saturated spots' intensity while the  $\times$ -symbols give an accurate estimate for the non-saturated spots' intensity. High-intensity spots at shortest exposure (5.6 s) may suggest a  $\sim 2$  times intensity overestimate for the short exposures while using the steady-source approach. However the statistics in Fig. 3 are not good enough (both because of saturation and because many lightning images are not sensitive to faint spots) to make a reasonable short-exposure intensity correction.

We also calculate the total power  $P$  of the several-pixel-wide lightning storms. Following Little et al. (1999) we treat each flash as a patch of light on a lambertian surface, so that both upward and downward fluxes were assumed to be  $\pi$  times the intensity, which gives the total power of  $2\pi$  times the intensity times the area of the emitting patch.

$$P = \sum_{\text{pix}} 2\pi I \cdot (\text{Pixel Area}), \quad (3)$$

where  $I$  is the intensity of each pixel above the background calculated in Eq. (2), pixel area is measured in the image plane and equals the square of the pixel size, and the sum is taken over all lightning spot pixels.

Table 1 shows the results of the calibration for the 29 Galileo storms. The powers calculated here and the powers, which we will calculate for Cassini lightning do not account for the emission angle. As a result, Table 1 underestimates the powers calculated in Little et al. (1999) by a factor of  $\cos(e)$ , where  $e$  is the emission angle measured from the local vertical. For their power estimates Little et al. (1999) use a direct geometric projection assuming lightning to be a flat horizontal light-emitting patch. More accurate consideration of a 3-dimensional light diffusion through the clouds above lightning (Dyudina et al., 2002) suggests smaller slant viewing correction factors compared to the direct geometric projection. The correction factor values in the 3-dimensional model can vary from unity (i.e., no correction needed) to the factor of  $\cos(e)$ . Several Cassini lightning events are observed near the limb and thus navigational uncertainties transform into large uncertainties in the emission angles. Because of the uncertainties in slant viewing correction, navigational uncertainties, and because Galileo and Cassini lightning flashes, both observed at a variety of emission angles, need to be compared, we make no geometric correction. We present uncorrected and probably underestimated powers in Table 1. Many of the lightning spots in Table 1 have several saturated pixels (as marked by the asterisks in the last column). Because of the saturation, the Table 1 powers at these spots are further underestimated, probably by up to a factor of a few.

Spatial resolution is critical for the lightning detection because only multiple-pixel spots can be identified as lightning and distinguished from cosmic rays hitting the detector. The spatial resolution for most Galileo flashes (Table 1, column 7) is similar to the 60–90 km/pixel Cassini resolution, with a few exceptions of high-resolution flashes at the end of the table.

It is important for the Galileo–Cassini statistical comparison that both surveys include areas observed at high and low emission angles. Most Galileo and Cassini images in the survey include a significant fraction of the jovian disk (frames being a quarter to half a jovian diameter across), images covering areas near the disk center and near the limb. Most of Cassini survey area is imaged at emission angles of  $50^\circ$ – $60^\circ$ . Galileo survey is taken at slightly lower emission angles, Galileo flashes imaged at  $\sim 50^\circ$  on average (see Table 1, column 9).

Figure 4 shows the set of the Galileo lightning spots which will be used to predict the number of detectable flashes per unit area for the Cassini camera. All Galileo storms in Fig. 4 are rescaled to the same resolution, each image box covering  $2800 \times 2800$  km. The actual resolution of the Galileo camera can be seen as the coarse pixels in the first several storms and finer pixels in the bottom two rows of boxes, storms 21 to C20(3). As can be seen in Fig. 4 most

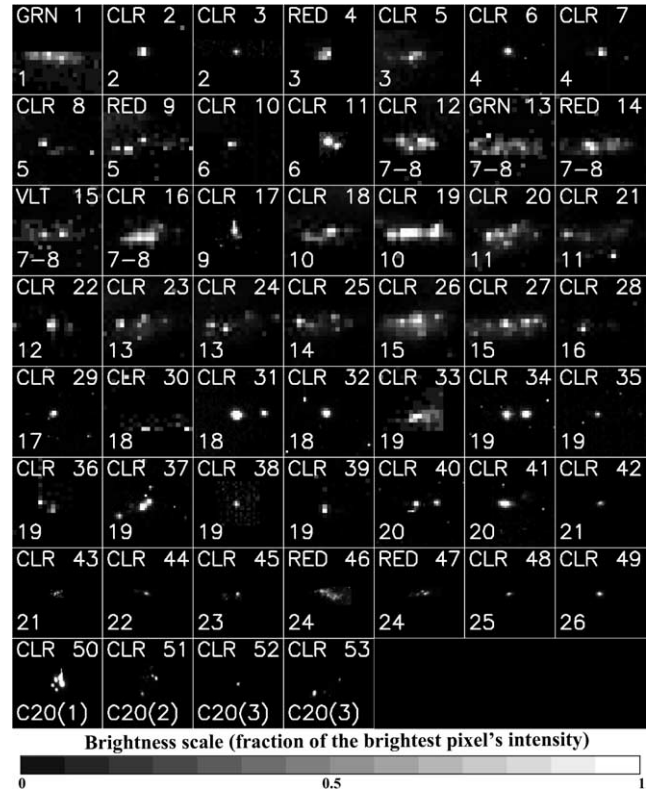


Fig. 4.  $2800 \times 2800$ -km-size boxes showing Galileo lightning observed on orbits C10, E11, and C20. The images are shown as they appear in the image plane and are not geometrically projected onto the jovian “surface.” The actual size projected onto the “surface” at emission angle  $e$  is foreshortened by a factor of  $\cos(e)$ . Brightness of each image is normalized by its brightest pixel. The number of the lightning spot (column 1 of Table 1) is labeled in the upper right corner of each box. The number of the storm according to Little et al. (1999) or the C20 storm number (column 2 in Table 1) is labeled in the lower left corner of each box. The filters are labeled at the upper left corners.

Galileo storms are larger than the largest (134 km) Galileo pixel size, and thus would be spatially resolved by the 60–90 km Cassini pixels provided the storms are bright enough for the Cassini camera.

The total area in the Little et al. (1999) C10–E11 Galileo survey is  $39.5 \times 10^9$  km<sup>2</sup>. We add  $\sim 1.1 \times 10^9$  km<sup>2</sup> of the C20 survey area to this number and obtain the combined C10, E11, and C20 survey area of  $40.9 \times 10^9$  km<sup>2</sup>, approximately 0.6 times the jovian surface. Note that Little et al. (1999) count repeated observations of the same area only once while estimating the survey area at each orbit (C10 or E11), and then add the areas for the two-orbit survey. We calculate the corresponding Galileo lightning frequency counting repeated observations of the storms only once, e.g., if Galileo observed a surface patch of  $10^9$  km twice, saw a lightning storm flashing both times, the frequency would be one twice observed storm divided by one twice observed patch, or 1 storm per  $10^9$  km. To obtain better statistics for Cassini we count each repeated survey area and each repeated lightning spot, or, for the example above, the frequency would be two sightings of the storm divided by the

Table 1  
The results for Galileo orbit C10, E11, and C20 lightning flashes

Lightning spot number	Storm number	Image	Line	Sample	Filter	Pixel size km	Exposure time s	Emission angle degrees	$I$ (brightest pixel) $W/(m^2 sr)$	Power W
1	1	s0416081400.r	396	228	GRN	133	179.0	57	$0.016 \times 10^{-3}$	$0.04222 \times 10^9$
2	2	s0416112945.r	336	229	CLR	134	6.40	52	$1.019 \times 10^{-3}$	$0.55345 \times 10^{9*}$
3	2	s0416113600.r	702	456	CLR	67	12.8	52	$0.127 \times 10^{-3}$	$0.03525 \times 10^9$
4	3	s0416092068.r	371	391	RED	133	179.0	57	$0.016 \times 10^{-3}$	$0.01058 \times 10^9$
5	3	s0416098000.r	387	186	CLR	133	89.6	52	$0.090 \times 10^{-3}$	$0.16061 \times 10^9$
6	4	s0416110600.r	685	407	CLR	67	12.8	51	$0.428 \times 10^{-3}$	$0.23706 \times 10^{9*}$
7	4	s0416110845.r	319	198	CLR	134	8.50	52	$0.499 \times 10^{-3}$	$0.33533 \times 10^9$
8	5	s0416090800.r	385	216	CLR	133	89.6	51	$0.077 \times 10^{-3}$	$0.07885 \times 10^9$
9	5	s0416092068.r	370	168	RED	133	179.0	52	$0.009 \times 10^{-3}$	$0.02303 \times 10^9$
10	6	s0416107945.r	328	196	CLR	134	6.40	50	$0.311 \times 10^{-3}$	$0.21735 \times 10^9$
11	6	s0416113600.r	682	37	CLR	67	12.8	58	$0.107 \times 10^{-3}$	$0.10424 \times 10^{9*}$
12	7–8	s0416079900.r	378	352	CLR	133	44.8	53	$0.112 \times 10^{-3}$	$0.29107 \times 10^{9*}$
13	7–8	s0416081400.r	359	236	GRN	133	179.0	50	$0.014 \times 10^{-3}$	$0.04655 \times 10^9$
14	7–8	s0416081768.r	360	227	RED	133	179.0	51	$0.090 \times 10^{-3}$	$0.17877 \times 10^9$
15	7–8	s0416082145.r	359	216	VLT	133	179.0	50	$0.035 \times 10^{-3}$	$0.08446 \times 10^9$
16	7–8	s0416083400.r	381	221	CLR	133	44.8	50	$0.156 \times 10^{-3}$	$0.37149 \times 10^9$
17	9	s0416113600.r	616	406	CLR	67	12.8	45	$0.431 \times 10^{-3}$	$0.22460 \times 10^{9*}$
18	10	s0416079900.r	301	319	CLR	133	44.8	40	$0.136 \times 10^{-3}$	$0.32612 \times 10^{9*}$
19	10	s0416083400.r	303	156	CLR	133	44.8	39	$0.146 \times 10^{-3}$	$0.54374 \times 10^{9*}$
20	11	s0416090600.r	300	127	CLR	133	89.6	39	$0.111 \times 10^{-3}$	$0.32827 \times 10^9$
21	11	s0416090800.r	298	116	CLR	133	89.6	39	$0.218 \times 10^{-3}$	$0.37201 \times 10^9$
22	12	s0416098000.r	216	386	CLR	133	89.6	33	$0.532 \times 10^{-3}$	$0.46713 \times 10^9$
23	13	s0416090600.r	214	214	CLR	133	89.6	26	$0.123 \times 10^{-3}$	$0.29306 \times 10^9$
24	13	s0416090800.r	213	206	CLR	133	89.6	25	$0.184 \times 10^{-3}$	$0.34234 \times 10^9$
25	14	s0416098000.r	84	93	CLR	133	89.6	16	$0.266 \times 10^{-3}$	$0.39194 \times 10^9$
26	15	s0416090600.r	83	104	CLR	133	89.6	15	$0.158 \times 10^{-3}$	$0.54574 \times 10^9$
27	15	s0416090800.r	82	91	CLR	133	89.6	16	$0.192 \times 10^{-3}$	$0.53798 \times 10^9$
28	16	s0416098400.r	101	207	CLR	133	89.6	38	$0.185 \times 10^{-3}$	$0.10218 \times 10^9$
29	17	s0416103100.r	170	722	CLR	67	12.8	50	$0.538 \times 10^{-3}$	$0.24925 \times 10^{9*}$
30	18	s0416098400.r	8	262	CLR	133	89.6	53	$0.048 \times 10^{-3}$	$0.04413 \times 10^9$
31	18	s0416101900.r	60	294	CLR	67	51.2	54	$0.077 \times 10^{-3}$	$0.10078 \times 10^{9*}$
32	18	s0416103100.r	81	225	CLR	67	12.8	55	$0.535 \times 10^{-3}$	$0.37769 \times 10^{9*}$
33	19	s0416098400.r	7	339	CLR	133	89.6	56	$0.022 \times 10^{-3}$	$0.04645 \times 10^9$
34	19	s0416101900.r	62	440	CLR	67	51.2	53	$0.084 \times 10^{-3}$	$0.08902 \times 10^{9*}$
35	19	s0416102100.r	87	415	CLR	67	12.8	54	$0.252 \times 10^{-3}$	$0.12224 \times 10^9$
36	19	s0416102345.r	66	204	CLR	133	8.50	54	$0.694 \times 10^{-3}$	$0.40401 \times 10^9$
37	19	s0416102900.r	59	376	CLR	67	51.2	54	$0.083 \times 10^{-3}$	$0.09045 \times 10^{9*}$
38	19	s0416103100.r	80	356	CLR	67	12.8	54	$0.058 \times 10^{-3}$	$0.03045 \times 10^9$
39	19	s0416103345.r	66	170	CLR	133	8.50	54	$0.711 \times 10^{-3}$	$0.30428 \times 10^9$
40	20	s0416101900.r	46	440	CLR	67	51.2	55	$0.083 \times 10^{-3}$	$0.04535 \times 10^{9*}$
41	20	s0416102900.r	39	371	CLR	67	51.2	56	$0.082 \times 10^{-3}$	$0.05983 \times 10^{9*}$
42	21	s0420824600.r	239	121	CLR	27	6.40	67	$0.163 \times 10^{-3}$	$0.01679 \times 10^9$
43	21	s0420829145.r	99	143	CLR	27	6.40	79	$0.033 \times 10^{-3}$	$0.00355 \times 10^9$
44	22	s0420472100.r	12	229	CLR	27	6.40	68	$0.609 \times 10^{-3}$	$0.05192 \times 10^9$
45	23	s0420815645.r	366	105	CLR	26	6.40	53	$0.124 \times 10^{-3}$	$0.01279 \times 10^9$
46	24	s0420793801.r	61	112	RED	23	166.0	59	$0.033 \times 10^{-3}$	$0.01721 \times 10^9$
47	24	s0420794201.r	72	85	RED	23	38.9	61	$0.212 \times 10^{-3}$	$0.02903 \times 10^9$
48	25	s0420824645.r	260	150	CLR	27	6.40	65	$0.198 \times 10^{-3}$	$0.01370 \times 10^9$
49	26	s0420815645.r	368	287	CLR	26	6.40	53	$1.524 \times 10^{-3}$	$0.17052 \times 10^9$
50	C20(1)	s0498109845.r	240	107	CLR	25	6.40	50	$1.360 \times 10^{-3}$	$0.92634 \times 10^{9*}$
51	C20(2)	s0498109845.r	263	247	CLR	25	6.40	50	$1.191 \times 10^{-3}$	$0.18966 \times 10^{9*}$
52	C20(3)	s0498094600.r	245	199	CLR	25	6.40	38	$0.629 \times 10^{-3}$	$0.02388 \times 10^{9*}$
53	C20(3)	s0498097145.r	222	295	CLR	25	6.40	53	$1.038 \times 10^{-3}$	$0.15523 \times 10^{9*}$

The asterisk (\*) in the last column denotes lightning spots with saturated pixels. The multi-observed storms (column 2) are numbered in the same order as in Little et al. (1999). The C20 in the second column marks the orbit C20 storms not described in Little et al. (1999). The pixel size is not corrected for the slant viewing geometry.

sum of the two sightings of the patch area, or 1 storm per  $10^9$  km. This should give lightning frequencies similar to the ones calculated for Galileo provided Galileo saw the same storms during the repeated observations. During the short time of each Galileo overlapped survey (up to 2 days for each orbit) most of the storms should still be active. Indeed many storms are seen by Galileo multiple times (column 2 in Table 1). Although Galileo images were targeted for lightning, the images were large, each covering large fraction of the planet, and the resulting Galileo area coverage is not substantially biased towards locations of unusually frequent lightning, as can be seen in Figs. 1 and 2 of Little et al. (1999).

The brightness detection limit for the Cassini camera can be determined from the Cassini lightning observations. Cassini images are routinely calibrated into the units of (photon  $\text{s}^{-1} \text{cm}^{-2} \text{sr}^{-1} \text{nm}^{-1}$ ) and also into the units of  $I/F$  (R. West, personal communication). The reflectance units of  $I/F$  are convenient when comparing the dayside and nightside brightness and we provide the  $I/F$  values together with intensities. The ‘ideal’ reflected intensity  $F$  is defined as intensity of the perfectly reflecting lambertian surface illuminated by the Sun at jovian orbital distance  $R_{\text{J}}$ . The value of  $F$  is  $1/\pi$  times the solar flux at  $H_{\alpha}$  wavelength,

$$F = \frac{1}{\pi} \int_{\text{HAL}} f_{\lambda}(R_{\text{J}}) \cdot T_{\text{HAL}}(\lambda) d\lambda, \quad (4)$$

where the solar flux  $f_{\lambda}(R_{\text{J}})$  is defined as the power of solar radiation intercepted by the unit area perpendicular to the beam per wavelength interval  $d\lambda$ , HAL denotes the Cassini  $H_{\alpha}$  filter, and  $T_{\text{HAL}}$  is the transmissivity of the filter.

We obtain intensities in units of  $\text{W}/(\text{m}^2 \text{sr})$  from the standard calibration of (photon  $\text{s}^{-1} \text{cm}^{-2} \text{sr}^{-1} \text{nm}^{-1}$ ) assuming the photons’ energy is  $h\nu_{0.65 \mu\text{m}} = 3.035 \times 10^{-19}$  J, and the effective width of the  $H_{\alpha}$  filter is 11 nm. We calculate the Cassini lightning power using Eq. (3), where  $I$  is the intensity above the background in the Cassini lightning spots. Because of the uncertainties in slant viewing correction, we do not account for slant viewing while calculating the powers of the storms. As a result, similarly to the Galileo estimates, the Cassini powers may be underestimated by a factor of up to  $\cos(e)$ , where  $e$  is the emission angle measured from the local vertical,  $60^{\circ}$ – $80^{\circ}$  for Cassini lightning.

Table 2 shows the calibration results for the four Cassini lightning clusters. Columns 6, 7, and 8 give the brightness in 3 ways—in dimensionless DN units, in dimensionless  $I/F$  units and in intensity units  $\text{W}/(\text{m}^2 \text{sr})$ . All flashes in Table 2 except Flash 4\* are multiple-pixel spots identified as lightning by their appearance. A single-pixel Flash 4\* is seen at the same location as Flash 3\* in the repeated observation of the same storm system (Flashes 3, 3\*, 4, 4\*) and thus believed to be lightning. Many other bright spots in the Cassini images are suspected of being lightning but are single pixels and thus cannot be distinguished from cosmic rays hitting the detector. Such small spots cannot be identified as lightning by either Galileo low-resolution images (all but the last

twelve in Table 1) or Cassini, and thus are not included in either set of lightning statistics.

Such unresolved lightning can contribute substantially to the global lightning flash rate and energy. An upper limit for single-pixel bright (above Cassini photometric sensitivity) lightning of order of  $10^3$ – $10^4$  events/planet follows from the fact that such lightning frequencies would be detectable globally because that number is comparable with the background cosmic ray frequency in the Cassini images. If lightning were present in such numbers, jovian disk would appear to have more one-pixel spots than the clear-sky background, where only cosmic rays, and not lightning are seen. However we do not see more one-pixel spots on the jovian nightside disc than on the clear sky.

Higher-resolution nightside (i.e., spacecraft-based) observations may help resolving small lightning spots. Another technique may help detect one-pixel lightning, namely defocussing the spacecraft’s telescope such that all real objects in the field of view are blurred by the telescope’s point spread function and thus are distinguishable from sharp-edged cosmic ray hits. Similar effect can be achieved by refining photometric resolution, such that each DN gives a smaller brightness step, and even the small blur of the telescope point spread function at the bright pixel’s edge is photometrically resolved and helps distinguish real objects from the cosmic rays. Refining photometric resolution would also help resolve faint lightning. The Cassini camera has an option of imaging in a fine photometric resolution mode (12 bits per pixel). However lightning observations on Jupiter were performed in a coarser photometric resolution mode (8 bits per pixel) due to technical difficulties during the flyby. The Cassini lightning search on Saturn is planned in full-resolution 12-bit mode.

Repeated observations of the same location taken by Cassini at Jupiter may help find “permanently flashing” one-pixel storms. However, this would require nearly one-pixel-accurate navigation. Currently such accuracy can only be reached with a priori known features, e.g., a limb, in the image frame to navigate the frame relative to these features. With few exceptions no such features are present in the Cassini lightning survey. In the case of Flash 4\* we used the repeated Flashes 3 and 4 for the relative navigation. Further development of absolute Cassini navigation may help identifying more single-pixel lightning in the data.

### 3. Results

#### 3.1. $H_{\alpha}$ line strength

First we will assume that the strength of the  $H_{\alpha}$  line,  $L_{H_{\alpha}}$ , corresponds to the laboratory simulation of lightning at 1 or 5 bars by Borucki et al. (1996) and will show that this is not consistent with the number of lightning detections observed by Cassini. Then we will argue that deeper lightning may explain the discrepancy.

Table 2  
Brightness results for the Cassini lightning spots

Image	Line	Sample	Pixel size km	Brightest pixel—backgr. DN/(I/F)/I 1/1/(W/(m <sup>2</sup> sr))	Background DN/(I/F)/I 1/1/(W/(m <sup>2</sup> sr))	Pix-to-pix noise DN/I 1/(W/(m <sup>2</sup> sr))	H <sub>α</sub> power W	
1	n1357029177.2	731	211	59.8	49/3.3 × 10 <sup>-3</sup> /7.4 × 10 <sup>-4</sup>	32/0.95 × 10 <sup>-3</sup> /2.1 × 10 <sup>-4</sup>	1/0.1 × 10 <sup>-4</sup>	0.413 × 10 <sup>9</sup>
2	n1357029177.2	846	397	59.8	37/2.4 × 10 <sup>-3</sup> /5.2 × 10 <sup>-4</sup>	33/1 × 10 <sup>-3</sup> /2.2 × 10 <sup>-4</sup>	1/0.1 × 10 <sup>-4</sup>	0.135 × 10 <sup>9</sup>
3	n1357810970.2	955	357	85.8	47/0.63 × 10 <sup>-3</sup> /1.4 × 10 <sup>-4</sup>	34/0.21 × 10 <sup>-3</sup> /0.5 × 10 <sup>-4</sup>	1/0.02 × 10 <sup>-4</sup>	0.263 × 10 <sup>9</sup>
3*	n1357810970.2	951	330	85.8	46/0.60 × 10 <sup>-3</sup> /1.41 × 10 <sup>-4</sup>	35/0.23 × 10 <sup>-3</sup> /0.49 × 10 <sup>-4</sup>	1/0.02 × 10 <sup>-4</sup>	0.072 × 10 <sup>9</sup>
4	n1357885387.2	775	341	89.4	34/0.45 × 10 <sup>-3</sup> /0.95 × 10 <sup>-4</sup>	36/0.24 × 10 <sup>-3</sup> /0.55 × 10 <sup>-4</sup>	1/0.02 × 10 <sup>-4</sup>	0.1 × 10 <sup>9</sup>
4*	n1357885387.2	775	316	89.4	71/1.18 × 10 <sup>-3</sup> /2.56 × 10 <sup>-4</sup>	36/0.24 × 10 <sup>-3</sup> /0.52 × 10 <sup>-4</sup>	2/0.04 × 10 <sup>-4</sup>	0.016 × 10 <sup>9</sup>

The brightest pixel values are given for multiple-pixel lightning clusters except Flash 4\*, a single pixel which is believed to be lightning because the spot is seen in two repeated observations at the same location (3\* and 4\* in Fig. 8). The  $I$  values are given together with DN's because the DN to  $I$  conversion is not linear for the Cassini camera and was performed using a lookup table (LUT). The pixel size is not corrected for the slant viewing geometry.

We invite the reader to judge whether a generic lightning spot (demonstrated on the example of 53 Galileo lightning spots) will be detectable by Cassini. We will progressively dim the 53 spots according to different H<sub>α</sub> line strengths and present the corresponding images compared to the Cassini noise level. We will count the number of detectable spots, divide it by the Galileo survey area and then try to match this Galileo-predicted lightning rate with the Cassini rate per unit area.

To estimate which of the Galileo flashes would be seen by Cassini, we will normalize the intensities of Galileo flashes by the brightest pixel of the faintest multiple-pixel spot in the Cassini survey that we identified as lightning. This is Flash 4 in Table 2 with the brightest pixel's intensity  $I = I_{\text{det}} = 0.95 \times 10^{-4} \text{ W}/(\text{m}^2 \text{ sr})$ , which is about  $34 \times$  the pixel-to-pixel noise level of 1 DN. Most of the pixels in Cassini Flash 4 are much fainter than 34 DN. Only because of these multiple faint pixels can we identify the spot as lightning and not as a cosmic ray hitting the detector. The image containing Flash 4 was taken during the second half of the Cassini survey. During the first half of the survey the photometric sensitivity was lower and the 1 DN intensity level was about 5 times coarser (see Table 2, column 8, Flashes 1, 2). Thus, for the first half of the survey,  $I_{\text{det}}$  corresponds to about 7 DN above the background. To demonstrate the Cassini detection limit, we rescale Galileo intensities such that the intensity from 0 to  $I_{\text{det}}/L_{\text{H}\alpha}$  appears in the image as the shades of gray (from black to white respectively) and an intensity of more than  $I_{\text{det}}/L_{\text{H}\alpha}$  appears white. After such rescaling, the bright flashes detectable by Cassini would appear as large bright spots, and the faint flashes undetectable by Cassini would be too faint to see as multiple-pixel spots.

Figure 5 shows such a prediction for the strength of the H<sub>α</sub> line corresponding to the 5-bar lab-simulated lightning (Borucki et al., 1996), i.e., when 16% of visible light falls within the H<sub>α</sub> filter. The Cassini pixel-to-pixel noise is about 1 DN, or 1/7 of  $I_{\text{det}}$  ( $I_{\text{det}}$  units are displayed on the brightness scale) for the first half of the survey. The pixel-to-pixel noise is 2.5–5 times smaller for the second half of the survey (see column 8 of Table 2). With such noise brightness variations of at least  $1/7 \times I_{\text{det}}$  would be resolved throughout the whole survey. As can be seen in Fig. 5 many of the

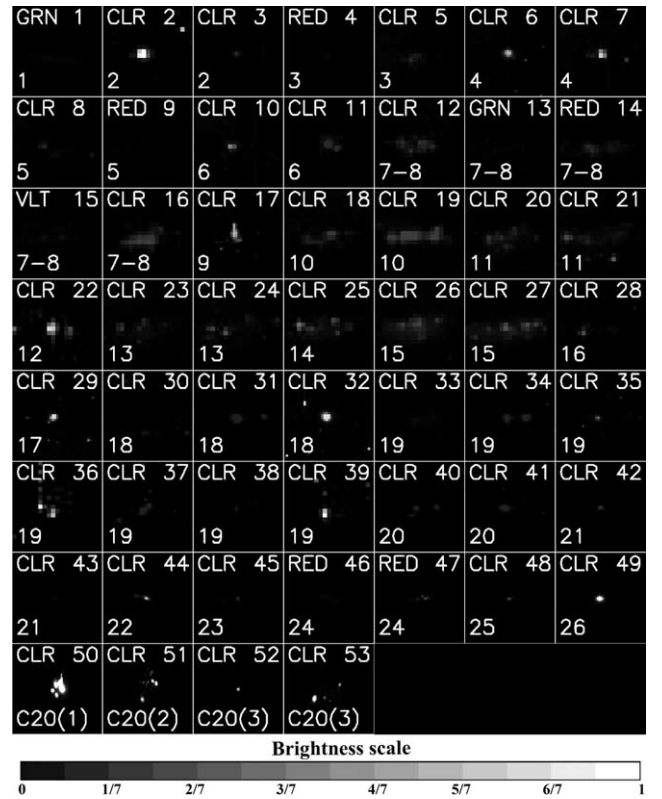


Fig. 5. Prediction for how Cassini camera would see the Galileo lightning if 16% of the light were emitted at H<sub>α</sub> wavelengths. The flashes are the same as in Fig. 4 except the intensities for all the flashes are normalized by the intensity of  $I_{\text{det}} = 0.95 \times 10^{-4} \text{ W}/(\text{m}^2 \text{ sr})$  divided by  $L_{\text{H}\alpha} = 0.16$  to account for the H<sub>α</sub> line strength.

Galileo storms are both bright enough and large enough for Cassini to have detected them if lightning originated from the 5-bar level. We consider the following storms (labeled in the lower left of each image box, see also column 2 of Table 1) detectable: 2, 4, 6, 9, 12, 17, 18, 19, 26, C20(1), C20(2), C20(3). Some of the Galileo flashes are saturated. The brightest pixels in these spots appear at saturation intensity, fainter than their actual intensity. Thus the number of detectable flashes may be underestimated. Dividing the 12 detectable storms above by the Galileo survey area of  $40.9 \times 10^9 \text{ km}^2$  we obtain one Cassini-detectable storm per

$\sim 3.4 \times 10^9 \text{ km}^2$ . Based on this number, Cassini should have seen about 60 lightning spots in its  $2.14 \times 10^{11} \text{ km}^2$  survey, some of them being the repeated views of the same storm. If we consider lightning at 1 bar instead of lightning at 5 bars and the corresponding  $H_\alpha$  line strength of 23% instead of 16%, the  $H_\alpha$  images would look brighter and even more storms should be seen. However, only 4 storms were actually detected by Cassini. One possible explanation is the lightning depth. As seen in Fig. 2, the  $H_\alpha$  line is broader for the 5-bar lightning than for the 1-bar lightning. Lightning deeper than 5 bars would produce an even broader  $H_\alpha$  line because of the pressure and temperature broadening deeper in the atmosphere. In this case the light seen through the  $H_\alpha$  filter will be fainter than 16% of the broadband light assumed above, fewer storms will be seen as multiple pixels and thus detected by Cassini.

To give a rough estimate for the  $H_\alpha$  line strength from the observations we estimate how many storms should be seen per Galileo survey area assuming the Cassini occurrence frequency. Four Cassini storms per  $2.14 \times 10^{11} \text{ km}^2$  survey give about 0.8 storms per Galileo survey area. If the lightning had a flat spectrum with no  $H_\alpha$  line the line strength would appear as the ratio of the CLR and  $H_\alpha$  filter widths,  $11 \text{ nm}/550 \text{ nm} = 0.02 = 2\%$ . This is a minimum line strength which we would expect in the case when the line emission is small compared to the broadband continuum emission in the lightning spectrum. To check this line strength against the observed number of lightning storms we make another prediction assuming  $L_{H_\alpha} = 2\%$ . Figure 6 shows the lightning brightness prediction for the  $H_\alpha$  line strength 2% constructed in the same way as we did before for the 5-bar line strength of 16% (Fig. 5). Figure 6 is consistent with the prediction of 0.8 storms per Galileo survey for the following reason. A few of the spots in the boxes (2, 32, 50) would appear several coarse pixels across at about 0.2, 0.1, and 0.3 of  $I_{\text{det}}$ , respectively (marginally-seen grey in Fig. 6). The brightness of these three spots corresponds to  $\sim 1$ , 1, and 2 DN's above the background for the first half of the Cassini survey. For the second half of the Cassini survey the brightness corresponds to  $\sim 7$ , 3, and 10 DN's. All of these spots are saturated and appear in Fig. 6 at the Galileo cut-off saturation intensity. Without saturation, the spots would appear brighter, probably at or above  $I_{\text{det}}$ , i.e., would appear white in Fig. 6, which corresponds to 7 DN for the first half of the Cassini survey and 34 DN for the second half of the Cassini survey. These few marginally-detectable spots may give a cumulative detection probability of 0.8 storms per Galileo survey area, as expected from Cassini data.

Figure 7 demonstrates why very strong lightning should be very rare on Jupiter. The figure shows a histogram for Galileo clear-filter lightning powers. The high-power tail shows decreasing frequencies for stronger lightning. Note that the actual distribution should be even more skewed than in Galileo observations because of the two observational biases. First, saturation makes the brightest lightning appear dimmer and thus some medium and high power lightning is

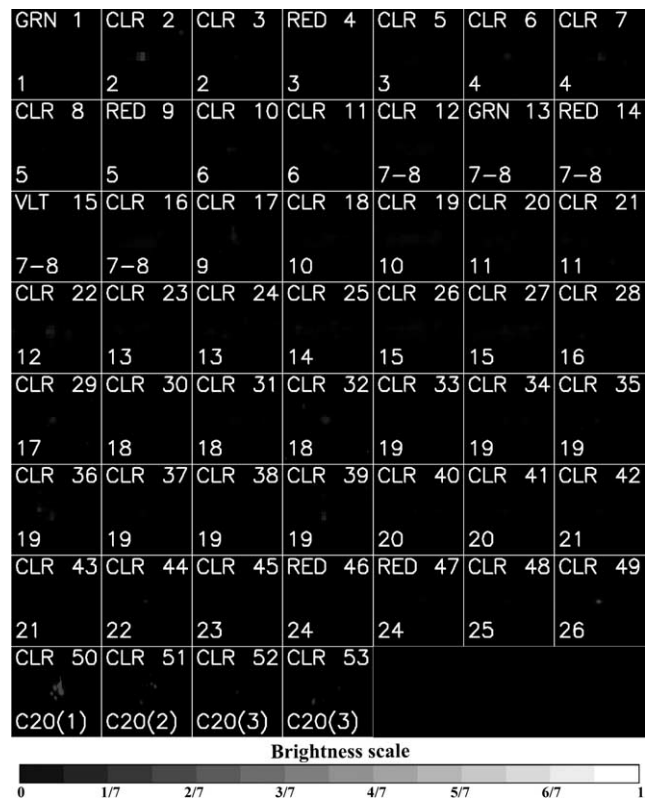


Fig. 6. Prediction for how Cassini camera would see the Galileo lightning if 2% of the light were emitted at  $H_\alpha$  wavelengths. The flashes are the same as in Fig. 4 except the intensities for all the flashes are normalized by the intensity of  $I_{\text{det}} = 0.95 \times 10^{-4} \text{ W}/(\text{m}^2 \text{ sr})$  divided by  $L_{H_\alpha} = 0.02$  to account for the  $H_\alpha$  line strength.

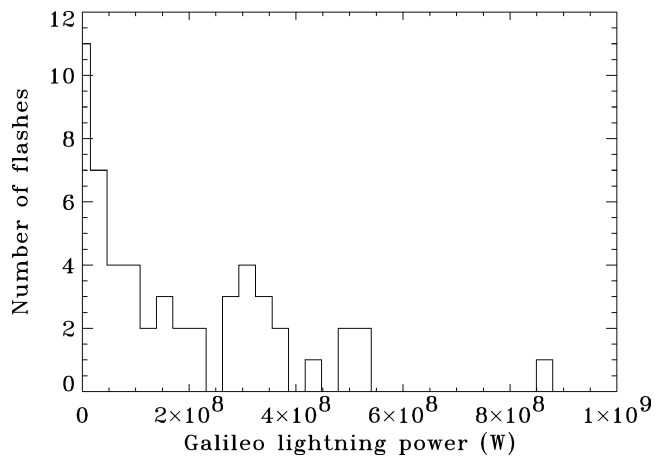


Fig. 7. Histogram of Galileo clear-filter powers (last column in Table 1).

actually more powerful than in Fig. 7. Second, low photometric sensitivity of some Galileo images prevents us from seeing the low-power events, which should be larger in numbers than in Fig. 7. Because of such biases the histogram can not be used to predict lightning frequencies at different power levels.

Bearing in mind the small numbers used for the storm statistics and the substantial variability in the high-power tail of

the lightning distribution on Jupiter and Earth (Uman, 1987), we estimate the lightning  $H_\alpha$  line strength to be 2% with an error bar of a factor of a few. This is consistent with a very weak, virtually absent  $H_\alpha$  line in the lightning spectrum.

The 2% estimate above is much smaller than the 16% line strength for the simulated 5-bar lightning. Thus, lightning deeper than 5 bars is a better explanation for the observed distribution than the shallow lightning. Lightning-producing charge separation on Jupiter is believed to occur in water clouds. Lightning deeper than 5 bars suggests that the water clouds themselves exist at depths more than 5 bars. The discharge may also occur between the cloud and the rain below the cloud. However, even on Earth with its conductive ground producing the effect of a “mirror” charge below the cloud and thus stimulating cloud-to-ground lightning, two thirds of the lightning occurs within the clouds and does not reach the ground. In the absence of the conductive surface all jovian lightning is likely to occur within the clouds (see discussion in Dyudina et al. (2002)). To support clouds at the depths of more than 5 bars and the corresponding temperatures, water abundance in the deep jovian atmosphere should be more than  $1 \times$  solar. Laboratory simulations of the lightning spectrum for pressures more than 5 bars may help to determine the deep jovian water abundance from our  $H_\alpha$  line strength.

At this point we must give a warning about our water abundance restriction. Our reasoning bears a number of assumptions. The least certain, in our opinion, are the following assumptions. We assume global planet-average lightning rate and the power-frequency spectrum to be steady on the timescales from few hours of each observation to few years between the Galileo and Cassini observations. We use small number of Cassini lightning for statistics. We assume water and not any other clouds to be responsible for lightning. We do not allow lightning to discharge into the rain below the cloud. Violation of any of these assumptions would alter our water abundance restriction.

### 3.2. Correlation between lightning and sunlit clouds

All four of the lightning spots observed by Cassini are correlated with unusually bright small ( $\sim 1000$  km in size) clouds on the day side. Such correlation is also seen in some images from Voyager 2 (Borucki and Magalhães, 1992) and Galileo (Little et al., 1999; Gierasch et al., 2000). The bright small clouds are quite rare, a few per planet at a time (Porco et al., 2003; Li et al., 2004) Visible and near IR spectra suggest that these clouds are dense, vertically extended, and contain unusually large particles (Banfield et al., 1998; Dyudina et al., 2001; Irwin and Dyudina, 2002), which is typical for terrestrial thunderstorms.

Figure 8 shows the day-side clouds (greyscale) overlain by the night-side lightning (red spots). The navigation (J. Spitale, personal communication) and the night/day image overlay are subject to an error less than  $2^\circ$ , one degree corresponding to about 1200 km. Not all of the red spots in

Fig. 8 are clearly-detected lightning. Some of the spots are suspected one-pixel cosmic ray hits indistinguishable from lightning. We did not eliminate these spots from the images because they may also be lightning.

Lightning in Voyager 2 (Borucki and Magalhães, 1992) observations are not always correlated with small bright clouds. Small bright convective-looking clouds in the Cassini dayside survey (Porco et al., 2003) are preferentially observed at low latitudes while lightning appears mostly at high latitudes in the Voyager and Galileo surveys. Because Cassini could observe very few, and only the most powerful lightning storms, the correlation of the clouds with Cassini lightning may suggest that only the most powerful thunderstorms with bright lightning penetrate the troposphere up to the levels where they are easily observable in reflected light. Fainter Voyager and Galileo lightning apparently does not always express itself in bright clouds because not enough clouds are seen at these latitudes to explain all the lightning. Note that the one-to-one correlation of Cassini clouds and lightning is observed on a rather small sample of simultaneous day and nightside observations. Detection of convective clouds is much harder at the high phase angles when the nightside observations are possible and the corresponding dayside crescent is small. As a result most of the convective clouds in Porco et al. (2003) are detected on full-phase Jupiter before the Cassini flyby. Very few of the clouds are detected after the flyby, when the nightside is seen and correlation with lightning can be explored.

Observation times are marked in Fig. 8 in black and red for the clouds and lightning images respectively. The two images on the right are repeated observations of the same storm in the turbulent wake of the Great Red Spot (GRS), with time separation of about 20 hr (2 jovian rotations). Clouds similar to this storm are known to appear and be sheared apart by the zonal winds on a timescale of 2–11 days. Li et al. (2004) find that the distribution of lifetimes follows a decaying exponential with a mean lifetime of  $\sim 4$  days. The 20-hr-long electrical activity of such storms suggests that lightning-producing convective updrafts are active for a substantial fraction of the storm’s lifetime. Remarkably, the most intense Galileo lightning C20(1) also occurred in the GRS wake. Apparently this region of unusually strong turbulent eddies in the atmospheric flow is favorable for unusually strong lightning.

Figure 9 shows the vertical structure of the storm clouds. Images taken by ISS at different wavelengths are sensitive to different depths. Figure 9 is combined from images at three different wavelengths such that the false color indicates clouds at different depths. For each location the three images are taken with a continuum filter (CB2), a weak methane absorption band filter (MT2), and a strong methane absorption band filter (MT3), and are combined as red, green, and blue brightness respectively. The CB2 filter is sensitive to all clouds down to  $\sim 5$ –10 bars, and thus areas with only deep clouds look red in Fig. 9. The MT2 band is sensitive to clouds with tops down to  $\sim 2$ –5 bars, and thus medium level

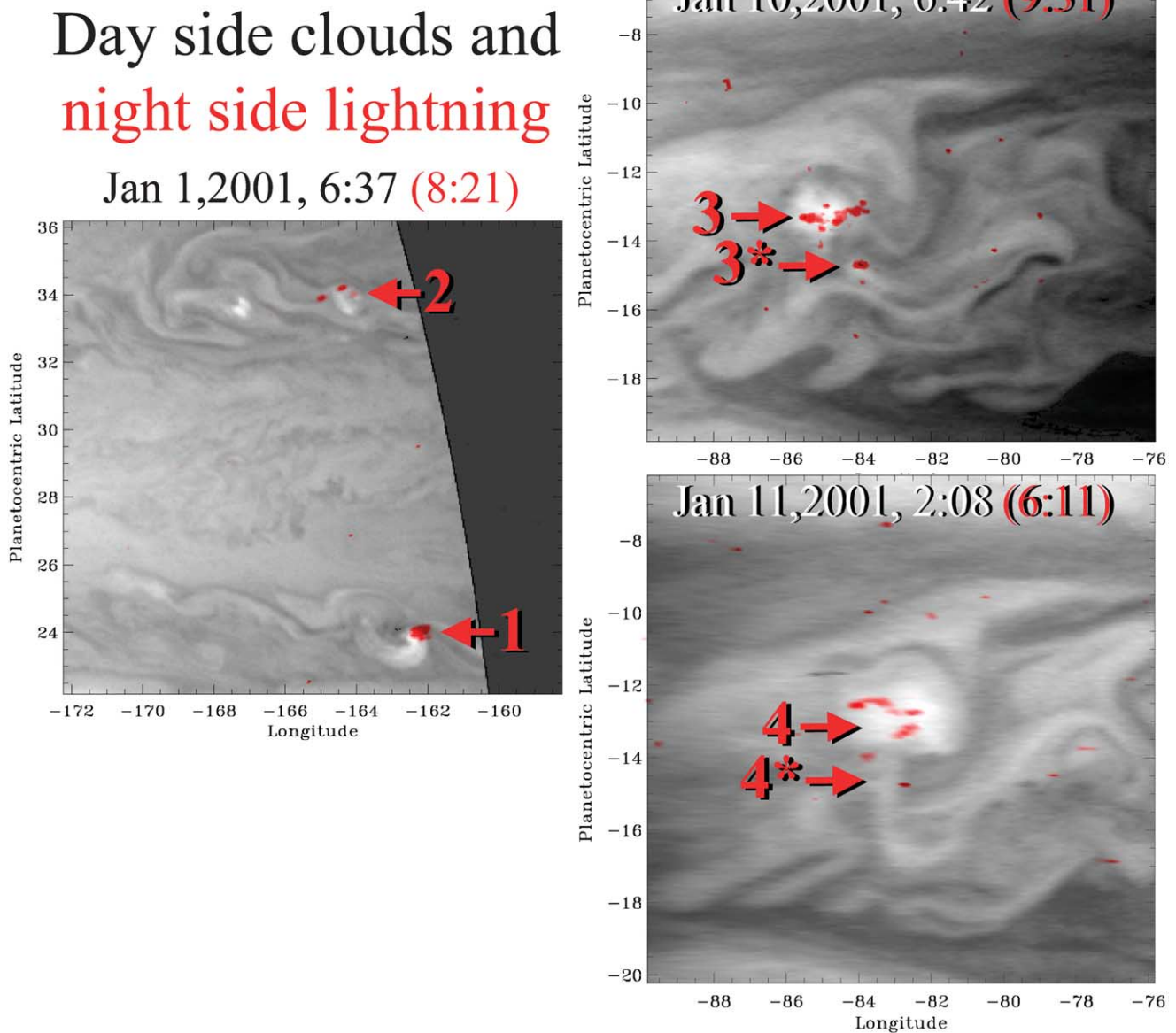


Fig. 8. Lightning on the night side of Jupiter (red) correlated with the clouds on the day side (greyscale) taken several hours earlier. Lightning spot numbers are labeled according to Table 2. The time is labeled on the images in red and black/white for the night side and the day side observations respectively. The image overlay and latitude/longitude scales are subject to a navigational error of less than  $2^\circ$ , one degree corresponding to about 1200 km. The red arrows point to the lightning spots listed in Table 2. The two images on the right display the same cloud in the turbulent wake of the Great Red Spot taken 2 jovian rotations apart.

clouds appear as shades of green. The MT3 band sees only clouds with high tops at  $\sim 0.1\text{--}0.5$  bars, near the tropopause, thus blue colors indicate hazes or cirrus above an otherwise cloudless troposphere (the deeper troposphere is dark in CB2 and MT2). White indicates clouds that are optically thick at all levels. Colors in Fig. 9 are only meaningful for comparison of clouds at small and medium distances from each other. The smooth edge-to-edge color change in the images is due to limb darkening in the raw images and not due to cloud elevation variations.

Large lightning storms look white in all three images in Fig. 9, indicating optically thick vertically extended con-

vective towers and probably storm cloud anvils. As had been noted before in Galileo (Banfield et al., 1998; Irwin and Dyudina, 2002) and other Cassini images (Porco et al., 2003), convective clouds often have deep roots. Such deep clouds can be seen in Fig. 9 as red areas near the white convective clouds. Repeated observation of lightning storms number 3\* and 4\* (see red arrows in Fig. 9) correspond to a red-colored deep cloud which does not have a white high cloud nearby. This confirms the Voyager conclusion (Borucki and Magalhães, 1992) that jovian thunderstorms may generate lightning even when the clouds do not extend to the top of the troposphere and expose themselves as bright

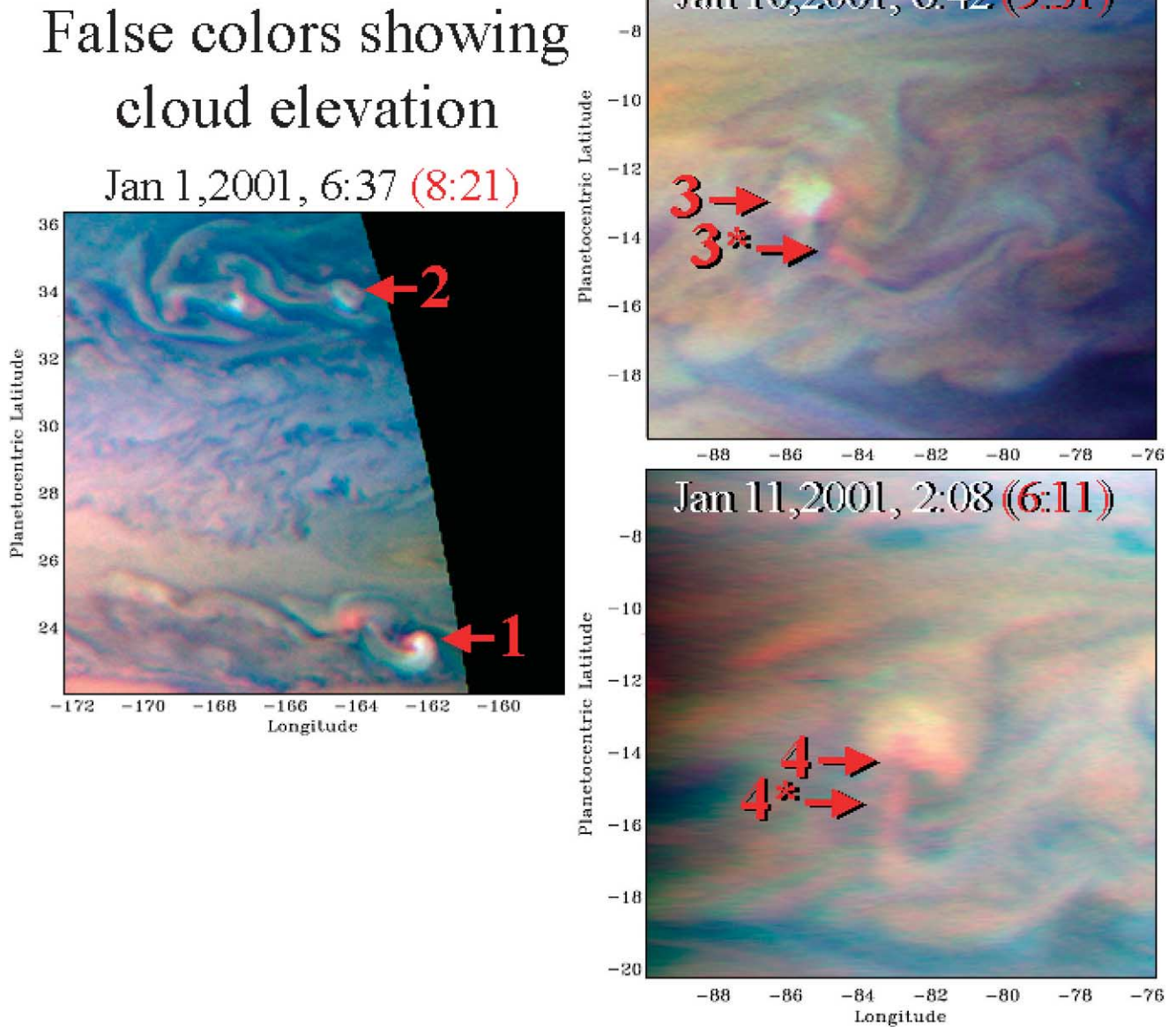


Fig. 9. False color images indicating heights of the clouds displayed in Fig. 8. The continuum (CB2), weak methane (MT2), and strong methane (MT3) images are loaded into the red, green, and blue color planes, respectively. January 1 image is combined from Cassini ISS frames n1357022884.1, n1357022921.1, and n1357022961.1. January 10 image is combined from frames n1357800891.1, n1357800928.1, and n1357800968.1. January 11 image is combined from frames n1357870836.1, n1357870873.1, and n1357870913.1. The red arrows indicate lightning storm locations as in Fig. 8. In this figure red color indicates deep clouds, green indicates intermediate clouds, blue indicates high hazes above otherwise cloudless troposphere. White clouds are optically thick at all levels.

clouds. These deep storms may develop the high tops several hours/days after or before this deep-thunderstorm stage, or they may remain at the deep levels during their entire lifetime.

Cassini lightning storms occur in 500- to 2000-km-size clusters. This is tens of times the size of the single flashes. Such clustering is also observed by Galileo (Little et al., 1999; Gierasch et al., 2000). The clustering is consistent with the 1000-km-scale uplifts created by the turbulent eddies in the jovian zonal atmospheric flow. The large-scale uplifts are favorable for a “forest” of convective plumes, each creating a fast 100-km-scale updraft which produces

repeated lightning, similar to the mesoscale convective systems on the Earth (Del Genio and Kovari, 2002). Similar scales are observed in Galileo jovian lightning clusters (Dyudina et al., 2002) and predicted in a mesoscale atmospheric flow model for the Voyager dayside convective clouds on Jupiter (Hueso et al., 2002).

### 3.3. Lightning power

Table 2 gives an estimate for the  $H_{\alpha}$  power of the lightning storms. The most powerful is Cassini Storm 1 emitting  $0.413 \times 10^9$  W in this narrow spectral band. This is about

half the  $\sim 0.9 \times 10^9$  W of the strongest Galileo clear-filter storm C20(1) (see the last column of Table 1). However, as in many of the Galileo storms, pixel values of the storm C20(1) are saturated and the power is underestimated, probably by a factor of a few. None of the Cassini lightning spots is saturated and the power estimate is more accurate than for Galileo. Because the Cassini Storm 1 power in Table 2 does not account for the slant viewing, the actual power at the emission angle of  $60^\circ$  may be a factor of 2 larger (see Section 2.1),  $\sim 0.8 \times 10^9$  W (similar slant viewing factor of 1.5–2 would be needed to calculate Galileo powers). We perform geometric correction to follow analogous corrections used previously for Galileo and Voyager energies. Rescaling this Cassini  $H_\alpha$  power to the broadband optical power with the  $H_\alpha$  line strength of  $L_{H_\alpha} = 2\%$  (derived above) will give  $(0.8 \times 10^9)/L_{H_\alpha} \approx 4 \times 10^{10}$  W with a factor of a few error inherited from  $L_{H_\alpha}$ .

The most energetic lightning was observed before by Voyager 2 in its  $2 \times 10^{10}$  km<sup>2</sup> survey (about 1/10 of Cassini survey) by Borucki and Magalhães (1992). To compare our powers with Voyager 2 powers we divide the Voyager 2 (420–900 nm) energies in Table IV of Borucki and Magalhães (1992) by the 95 s exposure time of these images. Thus we treat Voyager 2 storms as continuously flashing steady light sources. The resulting maximum optical power is  $3.4 \times 10^9$  W. It should be noted that the Voyager 2 lightning images were taken with a violet filter (380–485 nm) and the corresponding energies are converted to the broadband using a laboratory-simulated spectrum (Borucki and McKay, 1987). Cassini survey shows that powerful storms are very rare (order of 1 per planet at a time), and thus Galileo or the Voyagers may not have seen such powerful storms in their smaller surveys. The Galileo lightning power histogram (Fig. 7) suggests that, similarly to Earth (Uman, 1987), fainter lightning is much more frequent on Jupiter. Apparently with Cassini we see the very far high-energy tail of the lightning power statistical spectrum. Because Galileo highest lightning powers are underestimated due to saturation, we only compare Cassini powers with non-saturated Voyager powers. Provided Cassini lightning numbers are due to the lightning spectrum and not due to a long-term global weather change, and keeping in mind a factor of a few possible error inherited from  $L_{H_\alpha}$ , the Cassini Storm 1 has the largest optical power ever observed on Jupiter and is about 10 times stronger than the most intense storm witnessed by Voyager 2.

#### 4. Implications for lightning search on Saturn

Jupiter is the only planet other than the Earth where lightning had been unambiguously detected so far. After Cassini reached Saturn in June 2004, Cassini ISS started the search for lightning. It is extremely difficult to observe lightning on the dayside of any planet. For Saturn, all near-Earth telescopes can only look at the dayside. Only spacecraft beyond

Saturn's orbit can look at the night side and thus may detect lightning. The few attempts to image lightning on Saturn during the short Voyager 1 flyby were compromised by the light scattered by the rings (Burns et al., 1983). Cassini will have an unprecedented ability to discover lightning on Saturn. The spatial resolution will be as fine as 13 km/pixel. Because of the 12-bit ISS encoding the photometric sensitivity to the faint lightning on the bright background is an order of magnitude better than that of the Voyager cameras. Cassini will survey much more of the planet during many orbits than the Voyagers did during their short flybys.

The rings of Saturn create additional challenges for detecting lightning on Saturn relative to Jupiter. The light from the rings scattered in the camera and the planet's night side illuminated by the rings will produce substantial background brightness in the night-side images. Because the spectrum of saturnian lightning is expected to be similar to the jovian (Borucki et al., 1996), it was proposed to use the  $H_\alpha$  filter to combat the scattered light on Saturn, similarly to jovian observations. However, this strategy is efficient only when the  $H_\alpha$  line is sufficiently strong. Fewer lightning photons will reach the camera through the  $H_\alpha$  filter than through the clear filter and thus lightning will look fainter and may not reach the ISS intensity detection limit. Long exposures seemingly solve that problem by accumulating lightning intensities in the storm's area. However at long exposures storms will be smeared by the planetary rotation, and lightning will remain faint. This negative effect of using the  $H_\alpha$  filter is amplified when the  $H_\alpha$  line is weaker.

In this study we find that the  $H_\alpha$  line is fainter than expected for Jupiter (line strength of  $\sim 2\%$  instead of 16–23%), consistent with a flat lightning spectrum. If the lightning spectrum were flat, the  $H_\alpha$  filter would give virtually no advantage in fighting the scattered light as compared to the clear filter. Our  $\sim 2\%$  line strength has large error bars of a factor of a few. If the line strength is larger than  $\sim 2\%$  by this factor of a few, scattered light will be reduced when the  $H_\alpha$  filter is used instead of the clear filter. On Saturn the  $H_\alpha$  line is expected to be even weaker than on Jupiter because lightning-producing water clouds on Saturn are expected to exist at larger pressures (20 bars on Saturn versus 7 bars on Jupiter (Weidenschilling and Lewis, 1973)). Such a weak  $H_\alpha$  line (not more than the jovian  $\sim 2\%$ ) will give an even smaller advantage in avoiding scattered light.

Considering both the stronger negative effect and a smaller advantage of using the  $H_\alpha$  filter on Saturn we conclude that clear filter images, and not the  $H_\alpha$  filter images, are more likely to detect saturnian lightning. Thus it is more reasonable to perform large surveys targeted for discovery of faint lightning with the clear filter. However some  $H_\alpha$  filter night side images should be taken to study the spectrum of saturnian lightning and the  $H_\alpha$  line, which indicates the lightning depth.

Note that the reasoning above was based on the assumption that lightning on Saturn is similar to lightning on Jupiter. Although this similarity is our best guess, Saturn

may have substantially different lightning-generating mechanisms. Therefore a wide variety of observing strategies and filters, and not only the clear-filter large survey, may optimize discovery of saturnian lightning.

## Acknowledgments

We thank Joe Spitale for the help with navigating Cassini images and Kevin Beurle for the help with the ISS filter sensitivity. U.A.D. thanks Steve Desch for useful references and two anonymous reviewers for constructive critique. This research was supported by the NASA Cassini Project.

## References

- Banfield, D., Gierasch, P.J., Bell, M., Ustinov, E., Ingersoll, A.P., Vasavada, A.R., West, R.A., Belton, M.J.S., 1998. Jupiter's cloud structure from Galileo imaging data. *Icarus* 135, 230–250.
- Borucki, W.J., Magalhães, J.A., 1992. Analysis of Voyager 2 images of jovian lightning. *Icarus* 96, 1–14.
- Borucki, W.J., McKay, C.P., 1987. Optical efficiencies of lightning in planetary atmospheres. *Nature* 328, 509–510.
- Borucki, W.J., McKay, C.P., Jebens, D., Lakkapaju, H.S., Vanajakshi, C.T., 1996. Spectral irradiance measurements of simulated lightning in planetary atmospheres. *Icarus* 123, 336–344.
- Burns, J.A., Showalter, M.R., Cuzzi, J.N., Durisen, R.H., 1983. Saturn's electrostatic discharges: could lightning be the cause? *Icarus* 54, 280–295.
- Cook, A.F., Duxbury, T.C., Hunt, G.E., 1979. First results on jovian lightning. *Nature* 280, 794.
- Del Genio, A.D., Kovari, W., 2002. Climatic properties of tropical precipitating convection under varying environmental conditions. *J. Climate* 15, 2597–2615.
- Desch, S.J., Borucki, W.J., Russel, C.T., Bar-Nun, A., 2002. Progress in planetary lightning. *Rep. Prog. Phys.* 65, 955–997.
- Dyudina, U.A., Ingersoll, A.P., Danielson, G.E., Baines, K.H., Carlson, R.W., the Galileo NIMS and SSI Teams, 2001. Interpretation of NIMS and SSI images on the jovian cloud structure. *Icarus* 150, 219–233.
- Dyudina, U.A., Ingersoll, A.P., Vasavada, A.R., Ewald, S.P., 2002. Monte Carlo radiative transfer modeling of lightning observed in Galileo images of Jupiter. *Icarus* 160 (2), 336–349.
- Gierasch, P.J., Ingersoll, A.P., Banfield, D., Ewald, S.P., Helfenstein, P., Simon-Miller, A., Vasavada, A., Breneman, H.H., Senske, D.A., the Galileo Imaging Team, 2000. Observation of moist convection in Jupiter's atmosphere. *Nature* 403, 628–630.
- Goody, R.M., Yung, Y.L., 1989. *Atmospheric Radiation*. Oxford Univ. Press, New York, Oxford.
- Hueso, R., Sánchez-Lavega, A., Guillot, T., 2002. A model for large-scale convective storms in Jupiter. *J. Geophys. Res.* 107, 5075.
- Irwin, P.G.J., Dyudina, U.A., 2002. The retrieval of cloud structure maps in the equatorial region on Jupiter using a principal component analysis of Galileo/NIMS data. *Icarus* 156 (1), 52–63.
- Klaassen, K.P., Belton, M.J.S., Breneman, H.H., McEven, A.S., Davies, M.E., Sullivan, R.J., Chapman, C.R., Neukum, G., Heffernan, C.M., Harch, A.P., Kaufman, J.M., Merline, W.J., Gaddis, L.R., Cunningham, W.F., Helfenstein, P., Colvin, T.R., 1997. Inflight performance characteristics, calibration, and utilization of the Galileo solid-state imaging camera. *Opt. Eng.* 36, 3001–3027.
- Li, L., Ingersoll, A.P., Vasavada, A.R., Porco, C.C., DelGenio, A.D., Ewald, S.P., 2004. Life cycles of spots on Jupiter from cassini images. *Icarus* 172, 9–23.
- Little, B., Anger, C.D., Ingersoll, A., Vasavada, A.R., Senske, D.A., Breneman, H.H., Borucki, W.J., the Galileo SSI Team, 1999. Galileo images of lightning on Jupiter. *Icarus* 142, 306–323.
- Magalhães, J.A., Borucki, W.J., 1991. Spatial distribution of visible lightning on Jupiter. *Nature* 349, 311–313.
- Porco, C.C., West, R.A., McEven, A., Del Genio, A.D., Ingersoll, A.P., Thomas, P., Squyres, S., Dones, L., Murray, C.D., Johnson, T.V., Burns, J.A., Brahic, A., Neukum, G., Veverka, J., Barbara, J.M., Denk, T., Evans, M., Ferrier, J.J., Geissler, P., Helfenstein, P., Roatsch, T., Throop, H., Tiscareno, M., Vasavada, A.R., 2003. Cassini imaging of Jupiter's atmosphere, satellites, and rings. *Science* 299, 1541–1547. See also the Cassini images and movies at [http://ciclops.lpl.arizona.edu/ciclops/images\\_jupiter.html](http://ciclops.lpl.arizona.edu/ciclops/images_jupiter.html).
- Rakov, V.A., Uman, M.A., 2003. *Lightning: Physics and Effects*. Cambridge Univ. Press, Cambridge, UK.
- Smith, B.A., Soderblom, L.A., Johnson, T.V., Ingersoll, A.P., Collins, S.A., Shoemaker, E.M., Hunt, G.E., Masursky, H., Carr, M.C., Davies, M.E., Cook, A.F., Boyce, J., Danielson, G.E., Owen, T., Sagan, C., Beebe, R.F., Veverka, J., Storm, R.G., McCauley, J.F., Morrison, D., Briggs, G.A., Suomi, V.E., 1979. The Jupiter system through the eyes of Voyager 1. *Science* 204, 951–972.
- Uman, M.A., 1987. *The Lightning Discharge*. Academic Press, New York.
- Weidenschilling, S.J., Lewis, J.S., 1973. Atmospheric and cloud structures of the jovian planets. *Icarus* 20, 465–476.
- Williams, M.A., Krider, E.P., Hunten, D.M., 1983. Planetary lightning: Earth, Jupiter, and Venus. *Rev. Geophys. Space Phys.* 21 (4), 892–902.